AD-A050 051

MARTIN MARIETTA LABS BALTIMORE MD
COMBUSTION PROPERTIES OF HIGH DENSITY FUELS.(U)
NOV 77   J M BRUPBACHER, M T MCCALL

F/G 21/9.1

N00019-76-C-0683

UNCLASSIFIED   MML-TR-77-72C   NL

AD
A050051

END
DATE
FILMED
3 -78
DDC

MML 77-72c

COMBUSTION PROPERTIES OF HIGH DENSITY FUELS

John M. Brupbacher and
M. Thomas McCall

Martin Marietta Corporation
Martin Marietta Laboratories
1450 South Rolling Road
Baltimore, Maryland 21227

D D C

FEB 15 1978

F

November 1977

Final Report for Period
1 November 1976 - 31 October 1977

REPORT DOCUMENTATION PAGE		READ INSTRUCTIONS BEFORE COMPLETING FORM
1. REPORT NUMBER (14) MML-TR-77-72c ✓	2. GOVT ACCESSION NO.	3. RECIPIENT'S CATALOG NUMBER
4. TITLE (and Subtitle) (6) COMBUSTION PROPERTIES OF HIGH DENSITY FUELS.		5. TYPE OF REPORT & PERIOD COVERED (9) Final Report 1 Nov 76 through 31 Oct 77
		6. PERFORMING ORG. REPORT NUMBER
7. AUTHOR(s) (10) John M. Brupbacher and M. Thomas McCall		8. CONTRACT OR GRANT NUMBER(s) (15) N00019-76-C-0683
9. PERFORMING ORGANIZATION NAME AND ADDRESS Martin Marietta Laboratories ✓ 1450 South Rolling Road Baltimore, Maryland 21227		10. PROGRAM ELEMENT, PROJECT, TASK AREA & WORK UNIT NUMBERS N00019-77-PR-RK004
11. CONTROLLING OFFICE NAME AND ADDRESS Naval Air Systems Command Code AIR-310C Washington, D. C. 20361		12. REPORT DATE (11) November 1977
		13. NUMBER OF PAGES 32 (12) 35 P.
14. MONITORING AGENCY NAME & ADDRESS(if different from Controlling Office)		15. SECURITY CLASS. (of this report) Unclassified
		15a. DECLASSIFICATION/DOWNGRADING SCHEDULE

16. DISTRIBUTION STATEMENT (of this Report)

APPROVED FOR PUBLIC RELEASE: DISTRIBUTION UNLIMITED

DDC FEB 15 1978 F

17. DISTRIBUTION STATEMENT (of the abstract entered in Block 20, if different from Report)

18. SUPPLEMENTARY NOTES

19. KEY WORDS (Continue on reverse side if necessary and identify by block number)

Ramjet	Ignition delay
Fuels	Combustion
RJ-5	Exo-tetrahydrodicyclopentadiene
Fuel additives	

20. ABSTRACT (Continue on reverse side if necessary and identify by block number)

A novel experimental technique has been developed to simulate combustion of liquid propellants in rocket engines. The method uses an ultrasonic nebulizer coupled to the downstream end of a shock tube, which is equipped with visible, infrared, and pneumatic monitoring devices. This system was used to initiate RJ-5 mist combustion in oxygen at around 1500°K with an associated reflected shock pressure of about 2 atm. Under these conditions, the ignition delay of RJ-5 droplets with a mean particle diameter of about 30 μ was 200 μsec, whereas

ignition delay of RJ-5 vapor in the same experiment was very short (<1 μsec). The droplet ignition delay decreased with increasing temperature and was approximately 100 μsec at 1700°K.

TABLE OF CONTENTS

ACCESSION for

NTIS	White Section	☑
DDC	Buff Section	☐
UNANNOUNCED		☐
JUSTIFICATION		

BY
DISTRIBUTION/AVAILABILITY CODES
Dist. | | SPECIAL

A

1

LIST OF ILLUSTRATIONS

2

INTRODUCTION

The proposed fuel, RJ-5, is a blend of several fused ring hydro-carbons of low carbon/hydrogen ratio. This feature of the fuel gives rise to a high density compared to the simple non-cyclic hydrocarbons which predominantly constitute JP-type fuels. The high density of the RJ-types, along with their high energy content, imparts to them a large volumetric heat of combustion, thus making them promising candidates for volume-limited tactical weapon systems. Typical components of the fuel are shown in Figure 1.

I   II   III
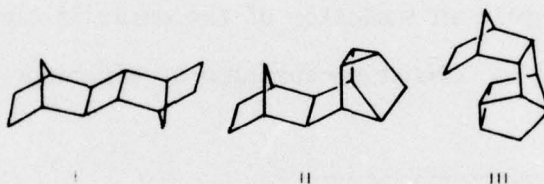
Figure 1. Typical components of RJ-5

The effect of structural differences on the combustion characteristics of RJ-5 is unknown. Furthermore, work is still in progress to improve the physical properties of the fuel by variation of the isomer ratio and/or by the addition of additives[1]. It is well established that small quantities of additives can have major effects on combustion parameters such as flame

(1)   A. Schneider, et al., "Air-Breathing Missile Fuel Development," Sun Oil Company, Contract No. F33615-73-c-2022, and related contracts, 1975 to date.

3

velocity[2], first and second ignition delays[3], and hot-wire ignition temperatures[4]. Many of these effects are difficult to predict a priori and to explain a posteriori.

Three prior studies on the combustion kinetics of RJ-5 have been carried out by Shell[5], Esso[6], and Martin Marietta Laboratories (MML)[7]. The goals of these preliminary studies were to: (1) investigate the effect of reaction conditions on the ignition delay (τ), and (2) determine the influence of viscosity-reducing additives. While extensive data on the variation of τ were obtained with the experimental techniques employed, it is not clear how these data would correlate with engine test firing results because τ is merely an indicator of the onset of combustion and is not directly related to combustion duration or efficiency.

(2)   H.G. Wagner, "Studies of Inhibitors as Anticatalytic Extinction
        Agents (Preliminary Report)," Research Contract No. 3155 (1955).

(3)   B. Lewis and G. von Elbe, Combustion, Flames and Explosions of
        Gases, 2nd Ed., Chapter IV, Academic Press, New York (1961).

(4)   M.E. Morrison and K. Scheller,"The Effect of Burning Velocity
        Inhibitors on the Ignition of Hydrocarbon Oxygen-Nitrogen Mixtures,"
        Combust. Flame 18, 1 (1972).

(5)   Shell Oil Company, Final Report Part II, AF APL TR 76-114 (1967).

(6)   V.J. Siminshi and F.J. Wright, Paper No. 72-71 presented at the
        AIAA 10th Aerospace Science Meeting, San Diego, California,
        January 17-19 (1972).

(7)   M. McCarty, Jr., J.N. Maycock, and D. Skean, "A Shock Tube Study of
        the Combustion of Shelldyne-H with Additives," presented at Western
        States Section/The Combustion Institute, Monterey, California,
        October 30-31 (1972).

Because of the uncertainties associated with ignition delay measurements, a more extensive study was carried out at MML[8], supported by the Naval Air Systems Command, with the aim of establishing a method for monitoring the entire combustion profile rather than just fuel ignition. This study showed that the infrared-coupled shock tube could yield valuable information on RJ-5 vapor combustion under homogeneous gas phase conditions. For instance, it was demonstrated that the burn rate increased with increasing temperature, with an apparent activation energy for combustion of 18 kcal/mol over the temperature (1900-3600°K) and pressure (1-1.5 atm.) range investigated. Furthermore, the study demonstrated that burn rate of RJ-5 vapors increased with both fuel and oxygen concentration but was unaffected by total gas pressure. It was also shown that the combustion rate depended only weakly upon the fuel isomer ratio. However, the combustion kinetics of a possible viscosity-reducing blending component, exo-tetrahydrodicyclopentadiene (exo-THDCPD), exhibited complex behavior under similar reaction conditions, suggesting that the behavior of RJ-5/exo-THDCPD blends might also be complex. The influence of this factor in real systems is still uncertain.

While this shock tube study provided much more information on the combustion kinetics of RJ-5 vapor than that obtained from ignition delay measurements, the results obtained could not be related to combustion in rocket engines where combustion is heterogeneous, i.e., fuel is introduced as a liquid into a hot combustion zone. The overall combustion process is, therefore, influenced by such parameters as rates of heat transfer and

(8)   John Brupbacher, M. Thomas McCall, and Maclyn McCarty, "Combustion of High Density Fuels," Martin Marietta Laboratories Final Report, MML TR 76-91c (1976).

5

vaporization of the fuel, and gas dynamics, as well as by the combustion kinetics of the homogeneous vapor phase.

Because of the difficulties associated with extracting meaningful combustion data from ignition delay measurements or from homogeneous vapor phase combustion profiles, the present study has been undertaken with the aim of developing a laboratory technique capable of more closely simulating combustion in real systems. The approach taken was the nebulizer-coupled shock tube in conjunction with infrared and visible monitoring techniques.

EXPERIMENTAL APPROACH

A number of approaches have been used for the study of hydrocarbon combustion, including use of laboratory flames, engine combustors, flow systems, and shock tubes. The difficulties in obtaining kinetic data from each of these devices vary considerably and involve such factors as heterogeneous reactions, finite heating duration, and temperature, pressure, and density gradients throughout the reaction zone. The approach that seems to present the fewest obstacles and to offer the greatest versatility is the chemical shock tube, which was therefore chosen for the present study. With the shock tube, premixed fuel-air mixtures can be rapidly heated to temperatures above the fuel autoignition temperature, whereby ignition and combustion will occur. Furthermore, the physical properties of the gaseous mixture can be readily varied to simulate a wide range of combustor conditions. When the chemical shock tube is used in conjunction with a technique that produces a fine liquid mist, a heterogeneous combustion environment is produced, which more accurately simulates combustion in rocket engines than the laboratory techniques presently used. The misting technique selected was an ultrasonic nebulizer. A description of shock tube and nebulizer operation follows.

Shock Tube

The chemical shock tube used in this program consists of two segments of pipe separated by a diaphragm. The first portion, the driver section, contains gas at a higher pressure than the second section. The driven section contains the gas mixture to be studied (e.g., RJ-5 + air). When the diaphragm is broken, either by bursting due to overpressure or by mechanical puncture, the driver gas expands into the driven section,

compressing and heating the gaseous mixture. The shock wave travels down the tube at supersonic speeds, sweeping the reaction mixture with it and generating the incident shock wave. When the shock wave reaches the end of the tube, the gas cannot be further displaced, and a second shock wave is produced, which leads to additional heating and compression. This wave moves away from the end of the tube and is referred to as the reflected shock. Aside from having much higher temperatures and pressures, the reflected zone differs from the incident zone in that it is stagnant, i.e., the gas in the reflected zone has no net velocity along the tube axis.

As a first order approximation, the temperatures of both incident and reflected shock zones are determined by the pressure differential across the diaphragm. In practice, the actual shock conditions are calculated from the experimentally measured shock velocity, the initial driven gas temperature and pressure, and a knowledge of the temperature-dependent heat capacity profile for the driven gas. Temperature and pressure profiles for a typical shock experiment monitored at a point near the end of the tube are illustrated in Figure 2.

Generation of Fuel Droplets

The methods available for the production of aerosols include the spinning disk[9,10], La Mer[9,10], atomizer impactor[10], isolated droplet[11,12],

---

(9)   H.L. Green and W.R. Lane, Particulate Clouds: Dust, Smokes, and Mists, Van Nostrand, Princeton (1964).

(10)   K.T. Whitby, D.A. Lundgren, and C.M. Peterson, Int. J. Air and Water Pollut., 9 263 (1965).

(11)   N.R. Lindblad and J.M. Schneider,"Method of Producing and Measuring Charged Single Droplets,"Rev. Sci. Instrum., 38, 325 (1967).

(12)   J.R. Adam, R. Catanev, and R.G. Semonin,"The Production of Equal and Unequal Size Droplet Pairs,"Rev. Sci. Instrum., 42, 1847 (1971).
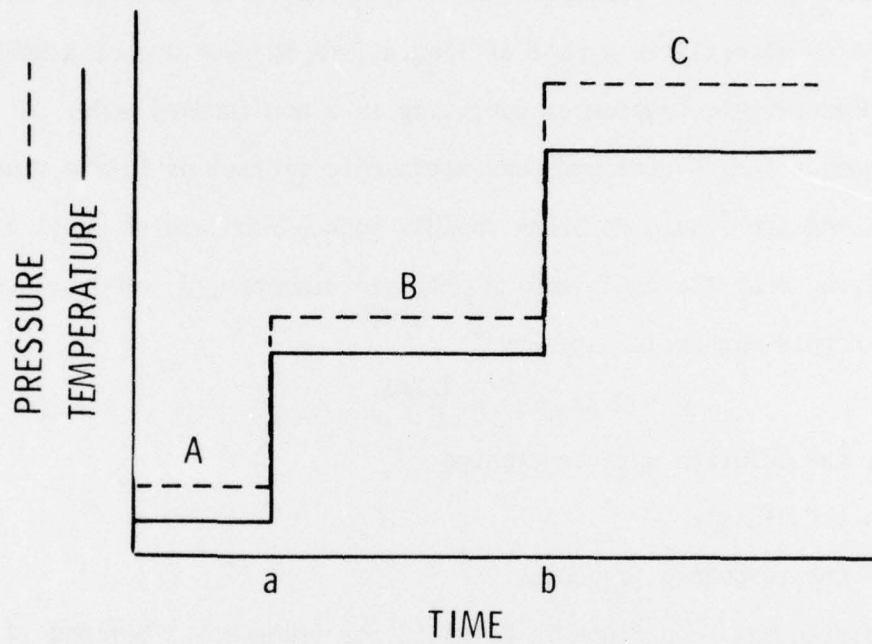
Figure 2. Temperature-pressure profile for shock tube experiment at a point near the tube end plate, showing incident and reflected shock conditions. Reaction zones are defined as follows:

A   Preshock conditions

B   Incident zone

C   Reflected zone

a   Incident shock arrival

b   Reflected shock arrival

and pneumatic generator techniques[13]. However, these methods produce only limited concentrations of aerosols or yield a wide distribution of particle sizes and are not readily suitable to shock-tube coupling.

In contrast, ultrasonic nebulizers have recently been developed that overcome these difficulties. With these devices, acoustical energy is transmitted directly to a pool of liquid from the surface of a barium titanate piezoceramic transducer operating in a non-focused mode. A radio frequency (RF) signal produces ultrasonic vibrations in the transducer, causing the liquid to break rapidly into a fountain of small drops. Lang has found that the count median particle diameter, d, of droplets produced in this manner is given by[14]

$$d = 0.35 \ (8\pi\sigma/\rho\omega^2)^{1/3}$$

where σ is the solution surface tension

ρ is the density

ω is the resonance frequency.

This expression has been found to be valid for frequencies between 12 kHz and 3 MHz, although there is some tendency for droplets to be smaller than predicted at frequencies above 1 MHz[15].

Furthermore, Denton, in adapting the ultrasonic nebulizer to the flame spectroscopic technique, has verified that the droplet size

(13)   J.A. Dean and W.J. Carnes, "Drop Size of Aerosols in Flame Spectro-photometry," Anal. Chem., 34, 192 (1962).

(14)   R.J. Lang, "Ultrasonic Atomization of Liquids," J. Acoust. Soc. Amer., 34, 6 (1962).

(15)   Yu. Ya. Boguslavskii and O.K. Eknadiosyants," Physical Mechanism of the Acoustic Atomization of a Liquid," Akust. Zh., 15, 14 (1969).

distribution is relatively narrow[16]. At 1 MHz, 90% of the droplets
produced were between 4 and 6 μ while 80% at 3 MHz were between 1 and
3 μ. The droplet size distribution curves for the aqueous solutions
examined by Denton are shown in Figure 3.
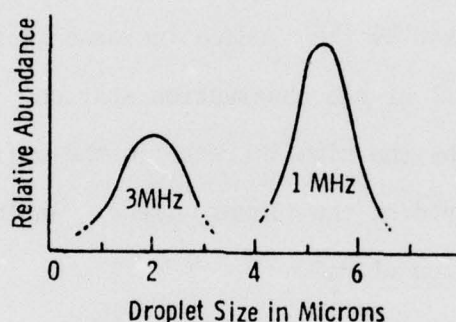
Figure 3. Droplet size distributions observed for 1 and 3 MHz operation

Larger droplets can be readily obtained with a lower RF frequency. The
nebulizing rate can be as high as 1 mℓ/min and depends only weakly upon
the solution depth. Also, the particle size distribution does not depend
strongly upon the nature of the solution, in agreement with theoretical
considerations.

Combustion Profiles

The species involved in the combustion process $RJ-5 + O_2 \longrightarrow$
$CO + CO_2 + H_2O$ have widely different physical properties, which make the
fuel well suited for analytical analysis. One property of the combustion
system, an intense infrared emission at high temperature, has been
chosen as a means of obtaining detailed, in situ, product profiles. The

(16)   M.B. Denton and D.B. Swartz, "An Improved Ultrasonic Nebulizer
        System for the Generation of High Density Mists," Rev. Sci.
        Instrum., 45, 81 (1974).

room-temperature absorption spectrum for the combustion system, shown
in Figure 4, demonstrates the ideal nature of this system for infrared
analysis. The fuel and both combustion products, CO_2 and H_2O, as well as
a product of incomplete combustion, CO, are well separated in the infrared.
A Polaroid ^{R} record of the infrared emission from CO_2 in a typical experi-
ment of RJ-5 vapor in air is seen in Figure 5. The sharp increase in the
shock tube pressure, marked by the sudden increase in the upper trace,
signals shock wave arrival at the observation station. Production of
CO_2 is clearly depicted by the slow increase in the infrared emission
(negative signal) displayed on the lower trace. Analogous profiles are
observed for the production of H_2O.
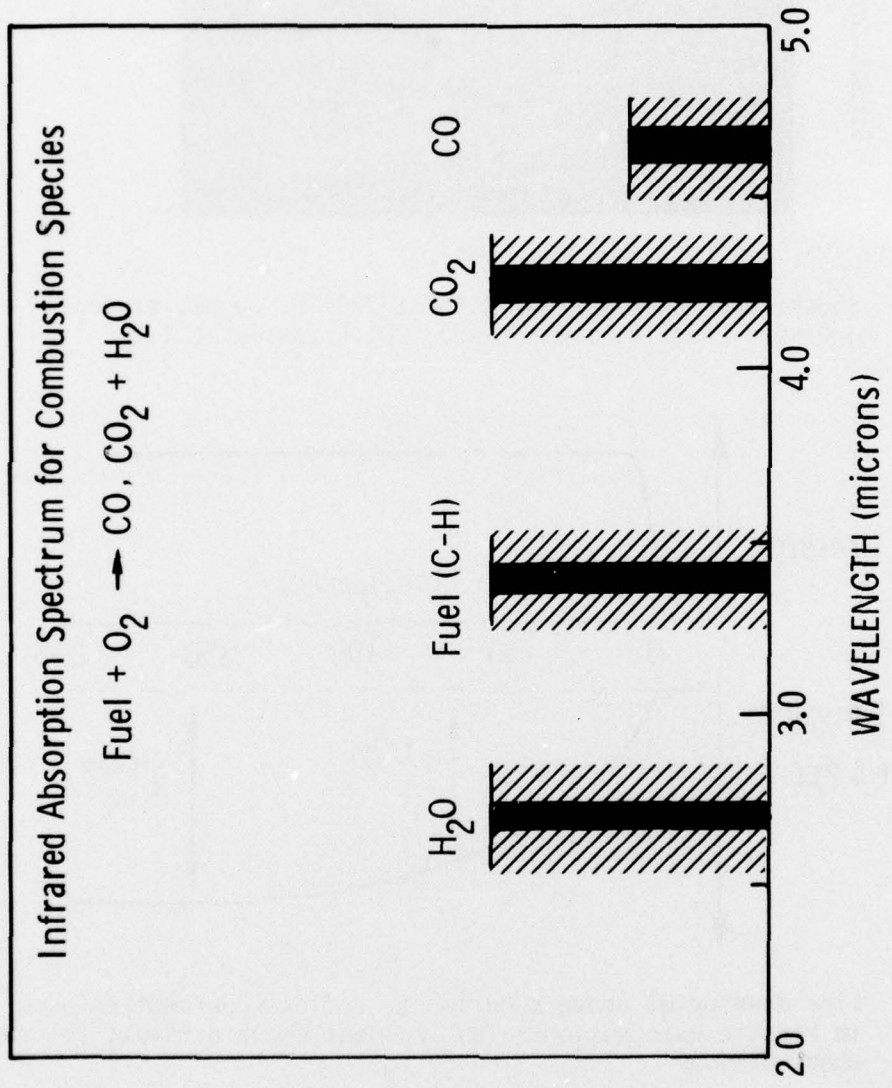
Figure 4. Room-temperature infrared absorption spectrum for combustion process, demonstrating well-separated absorption and hence, emission bands
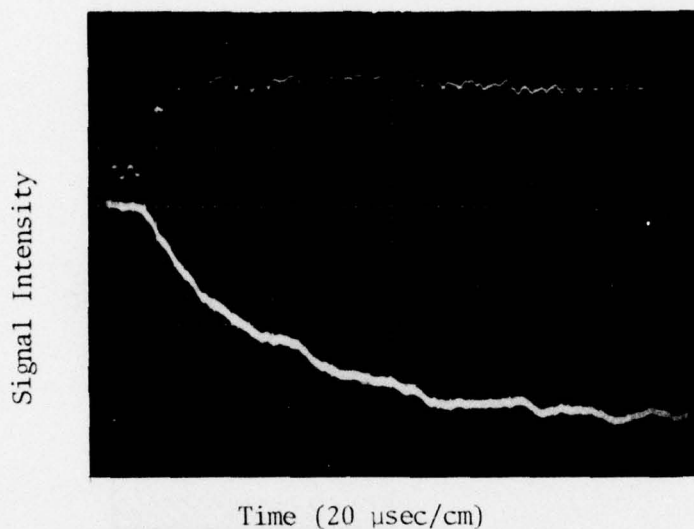
Figure 5a. Shock tube experiment of RJ-5 at $2200^{\circ}K$. Upper trace, pressure profile; lower trace, CO_2 emission at 4.2μ
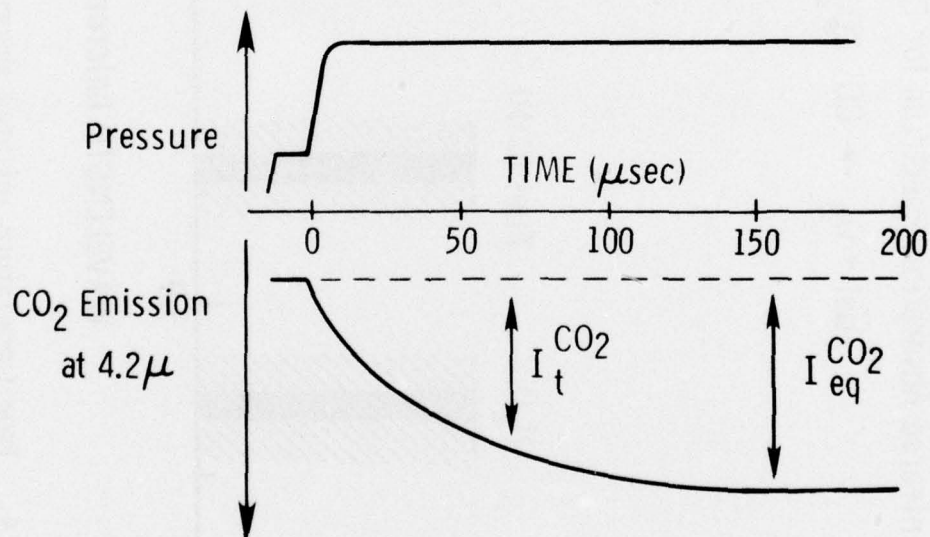
Figure 5b. Line drawing of above experiment, defining parameters used in kinetic calculations; (a) incident shock arrival; (b) reflected shock arrival

EXPERIMENTAL DESIGN

The existing shock tube system at Martin Marietta Laboratories proved to be inadequate for nebulizer coupling because of the short lifetime of the reflected shock zone. Consequently, a new shock tube system was designed and constructed. An overall view of the shock tube is shown in Figure 6, and a detailed drawing illustrating the combustion region is given in Figure 7. As before, the shock tube consists of two sections, a driver and a driven section, along with their associated control and monitoring devices. In the present application, the nebulizer constitutes a third major element. The three components are described below.

Driver Section

The driver or high-pressure section is constructed from a 32-liter stainless steel, military surplus oxygen bottle (500 psi) approximately 12 in. in diameter and 24 in. in length. A spring-loaded, double-bladed knife, installed into the driver section, ensures uniform and rapid diaphragm rupture. Diaphragm rupture is initiated by release of the cocked knife, which accelerates downstream and cuts the diaphragm in a quadrant petaling pattern. The knife is rapidly retracted from the foil region by spring tension, producing an unhindered path for driver gas expansion and, hence, a longer lifetime for the reflected zone. Aluminum diaphragms retain their post-shock configuration and readily exhibit the quadrant pattern. Also housed in the terminal knife mounting flange is a 1/2-in. port used for mechanical evacuation and as a driver gas (He) inlet. The entire driver section rests on a slide mounting frame so that it can be easily moved back for diaphragm changing. Pressure in the driver section is monitored on a 0-200 psi bourdon gauge.

15
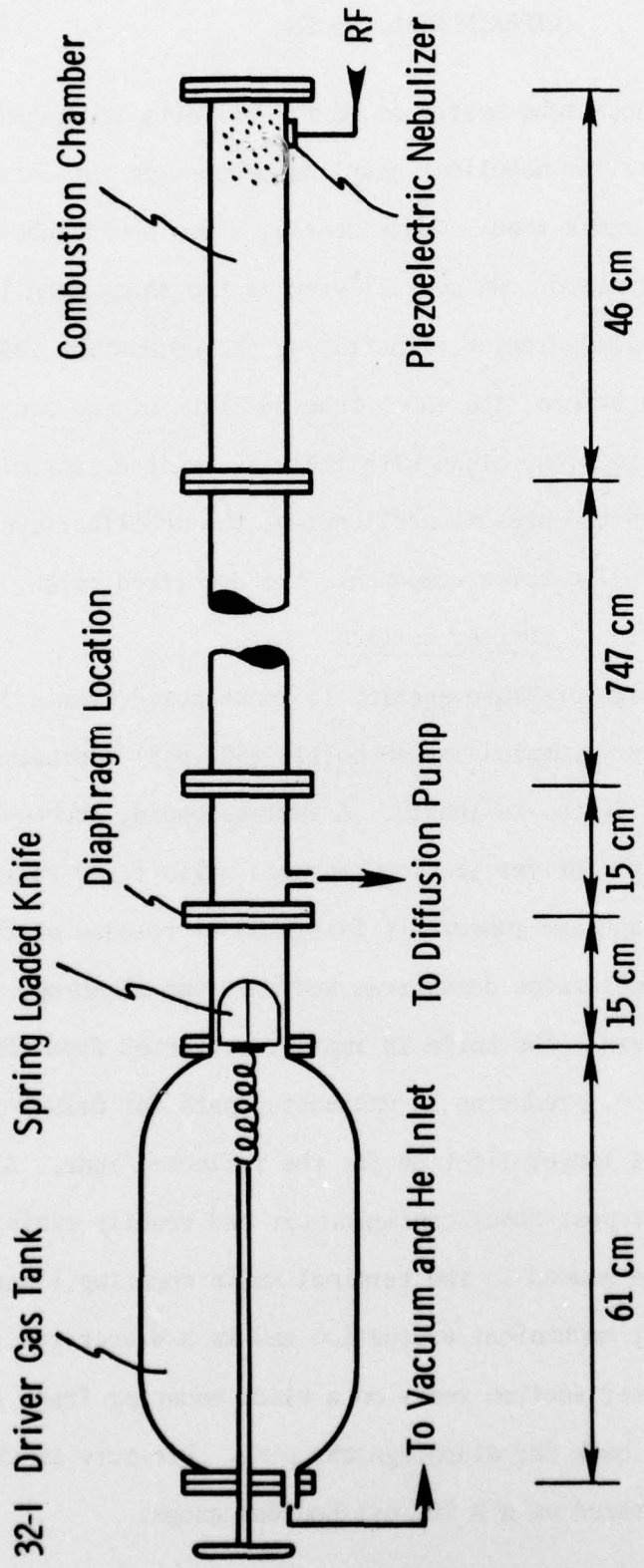
Figure 6.   General schematic of nebulizer-coupled shock tube

16
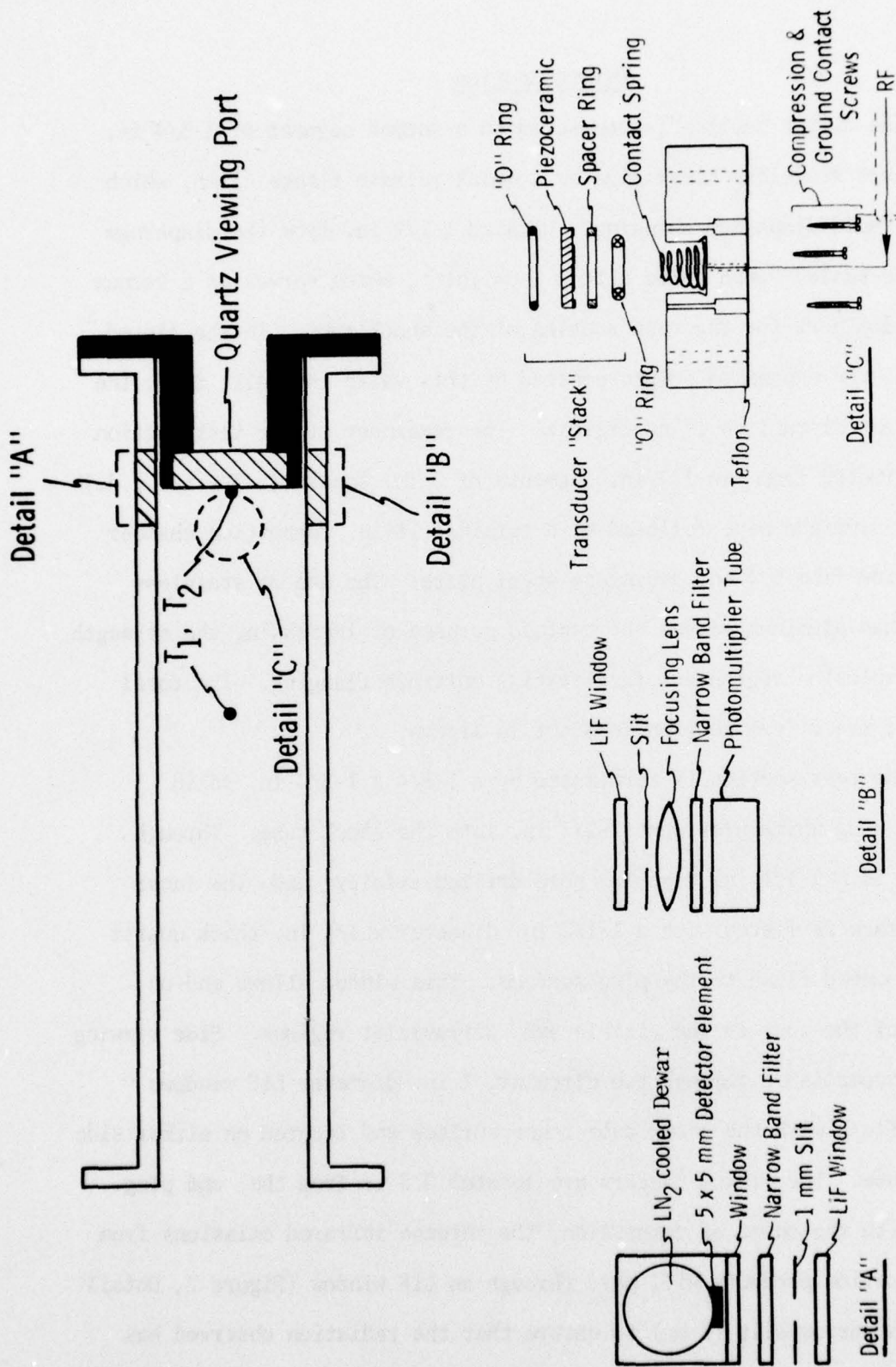
Figure 7. Detailed schematic of shock tube combustion zone

Quartz Viewing Port

Detail "A"

Detail "B"

Detail "C"

T_1, T_2

Detail "C"

"O" Ring
Piezoceramic
Spacer Ring
Contact Spring

Transducer "Stack"

"O" Ring

Teflon

Compression &
Ground Contact
Screws

RF

Detail "B"

LiF Window
Slit
Focusing Lens
Narrow Band Filter
Photomultiplier Tube

Detail "A"

LN_2 cooled Dewar
5 x 5 mm Detector element
Window
Narrow Band Filter
1 mm Slit
LiF Window

Driven Section

The driver section is connected to a second segment of 1-3/4 in. i.d. square stainless steel pipe by a quick-release flange clamp, which permits rapid diaphragm changing. Located 1-1/2 in. from the diaphragm is an end-sealed Veeco valve with a 1-cm inlet, which serves as a vacuum and filling port for the test section of the shock tube. In the closed position, the expansion volume created by this valve is small; thus, the shock-front disruption is negligible. The remainder of the test section is constructed from two 147-in. segments of 2-in. square (1-3/4 in. i.d.) seamless aluminum pipe followed by a terminal 18-in. combustion chamber constructed from 1/4-in. stainless steel plate. The use of stainless rather than aluminum serves the twofold purpose of increasing the strength in the explosion region and facilitating multiple flanging. The total volume of the driven section is about 16 liters.

The test section is terminated by a 1-3/4 x 1-3/4-in. solid aluminum plug which protrudes 1-1/2 in. into the shock tube. Through the plug is a 1-1/4-in. circular hole drilled axially, and the inner plug surface is fitted with a 1-1/2 in. diameter x 1/4 in.-thick quartz window mounted flush to the plug surface. This window allows end-on viewing of the zone in the visible and ultraviolet regions. Side viewing can be accomplished through two circular, 1 in.-diameter LiF windows mounted flush with the shock tube inner surface and located on either side of the tube. The window centers are located 0.5 cm from the end plug.

With the onset of combustion, the intense infrared emissions from the combustion products will pass through an LiF window (Figure 7, Detail A) onto a narrow slit (1 mm) to ensure that the radiation observed has

18

originated from a narrow slice of gas perpendicular to the tube axis. The unfiltered radiation emerging from the slit will pass through a narrow-band infrared filter with a characteristic transmission coincident with the emission of the species to be observed and finally impinge on the active element of an InSb infrared detector.

In a similar manner, the opposing window is equipped with a visible and ultraviolet monitoring device (Figure 7, Detail B). However, the active detecting device is a photomultiplier tube.

Located at positions T_2 and T_1, 0 and 10 cm from the end plug, respectively, are two pressure transducers. The shock velocity can be calculated from the sudden increase in pressure associated with the incident shock arrival at these two positions. This velocity determines the precombustion shock temperature. The rate of pressure change at T_2 also serves as a monitor of the fuel burn rate.

The gas handling system, attached to the test section near the diaphragm, consists of two 32-liter, stainless steel cylinders for gas mixture storage, 0-50 and 0-800 Torr absolute pressure gauges for mixture preparation, and a 2-in. oil diffusion pump. Vacuum measurements are made using an NRC vacuum monitor, which contains both the thermocouple and ionization gauges.

Nebulizer

Located on the bottom of the tube between the two side-viewing windows is a Channel Products ultrasonic transducer specifically designed for cavitating small volumes of liquids to create a fine mist. The transducer is mounted on the tube by a teflon flange which also houses a bronze spring and a spacer ring (Figure 7, Detail C). Pressure on the

19

transducer is generated by three compression screws that press against the spacer ring and serve as the second electrical contact to the transducer. The transducer resonance frequency and hence the mist particle size are inversely related to transducer thickness.

The piezoceramic transducer is driven by a radio-frequency power source[16] (Figure 8) capable of delivering over 100 W of energy over a frequency range of 700 kHz to 3.5 MHz. Irradiating power is controlled by the step resistors and potentiometer in the screen circuit of the output amplifier. Power is coupled to the piezoceramic transducer via a 0.01 µF, 4 kV transmitting mica capacitor, which isolates the high voltage plate supply from the transducer. The high-current, high-voltage D.C. power supplies were produced by modification of a Bendix Corporation Model 925 Knudsen cell power supply.

Located on the upper tube wall directly above the transducer is a rubber septum seal. This inlet allows direct introduction of a known amount of liquid fuel onto the crystal surface from a calibrated syringe.
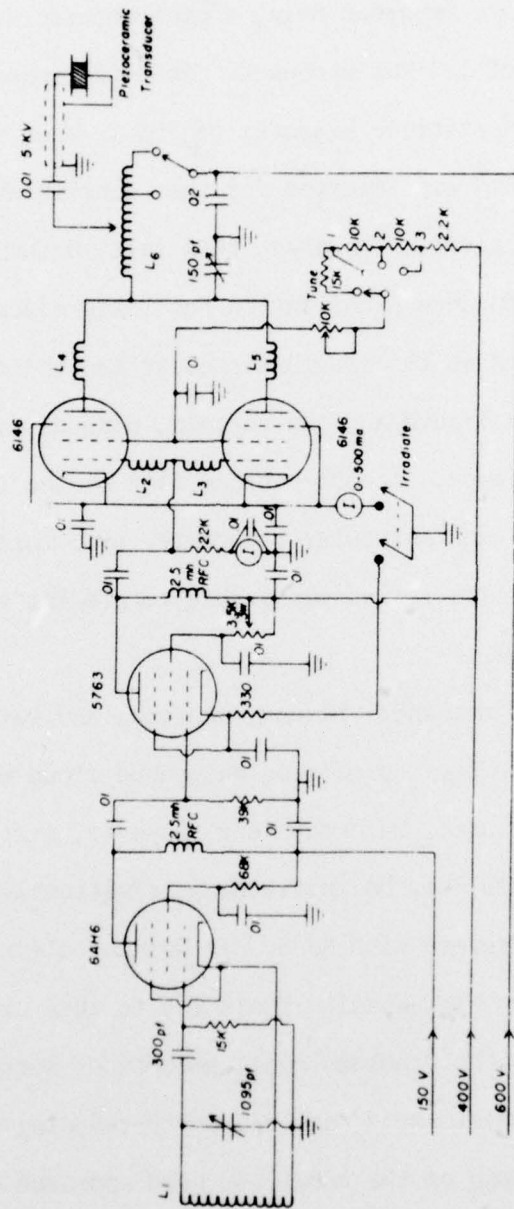
Figure 8. Schematic diagram [10] of the radio frequency source. Conventional radio frequency circuitry is employed to generate in excess of 100 W over a range of 700 kHz to 3.5 MHz.

RESULTS AND DISCUSSION

RJ-5 Mist Formation

In the experiments reported here, a piezoceramic transducer with a resonance frequency of 1.4 MHz was used. At this frequency, eq. (1) predicts a count median particle diameter of 2.6 μ when values of 1.08 gm/cm^3 and 39.4 $dynes/cm^2$ are inserted for the density and surface tension of RJ-5, respectively. However, this relationship only describes the droplet distribution once nebulization has taken place, when, in fact, many other factors, such as the liquid viscosity and the surface tension correlation between the liquid and the ceramic, play an important role in the nebulization efficiency. Acoustic properties of the liquid, determined by their chemical and molecular structure, also influence the efficiency. Unfortunately, it was impossible to predict the significance of these effects a priori.

Small samples of methanol, hexane, acetone, and water were placed on the oscillating transducer, producing an opaque cloud which emanated from the transducer surface. Unfortunately, however, mist formation with RJ-5 and exo-THDCPD could only be initiated intermittently. This difficulty was particularly severe with RJ-5. It was not clear what property of these two potentially high-density fuels led to this difficulty. In an attempt to alleviate the problem, small amounts of surface tension reducing agents, e.g., oleic acid, and viscosity-reducing agents, e.g., toluene, were added. None of the additives used appeared to improve mist formation.

Despite the difficulty in producing an RJ-5 mist, nebulization in the shock tube combustion chamber, located at the very end of the shock

22

tube, periodically yielded a mist that appeared to be relatively uniform throughout the last several inches of the shock tube and took about 15 seconds to completely settle. These properties were verified by a Tyndall-type experiment in which a narrow beam of light was directed along the shock tube axis. The perpendicularly scattered light from the small droplets was viewed through the side viewing ports, as shown in Figure 9. There appeared to be no tendency for the droplets to migrate to the shock tube walls or to agglomerate into larger drops.

A photograph of mist collected on a microscope slide passed through it is seen in Figure 10. Two features are readily apparent: first, the droplets are approximately of the predicted size (ca. 3 μ); second, the size distribution is very narrow, varying only a few microns from the largest to the smallest drop.

The mist generated in the combustion chambers in the experiment just described was produced at atmospheric pressure. However, the mechanics of the shock tube design precluded preshock pressures much above 50 torr lest the final reflected shock pressure exceed the safe operating limits of the combustion chamber. The mist produced at 50 torr tended to hover over the ceramic disk as a hemispherical cloud ≈ 1 inch in radius rather than distribute itself uniformly throughout the combustion region. This effect cannot be rationalized in terms of the "tranquil settling expression"[17].

$$C = \frac{gd^2(\rho_p - \rho_m)}{18\,\eta_m} \tag{2}$$

---

(17)   T. Yoshida, Y. Kousaka, and K. Okugama, Ind. and Eng. Chem. Fund., 14, 47 (1975).

23
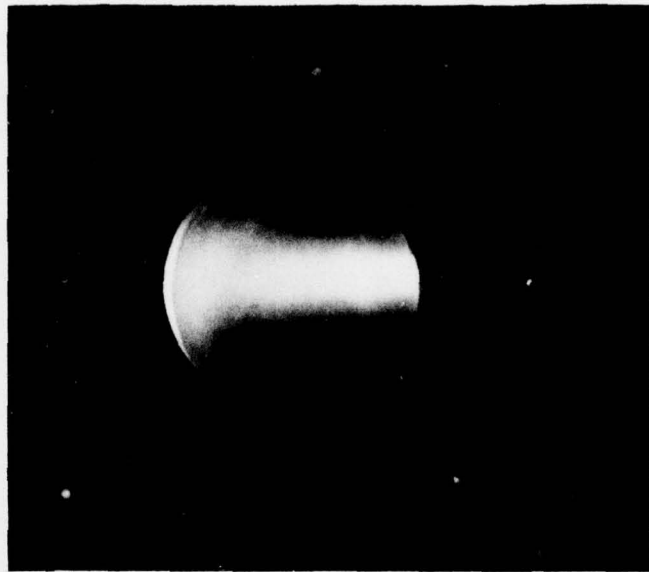
Figure 9.   Tyndall experiment of RJ-5 mist, photographed while nebulizing into beam of light introduced from end of shock tube
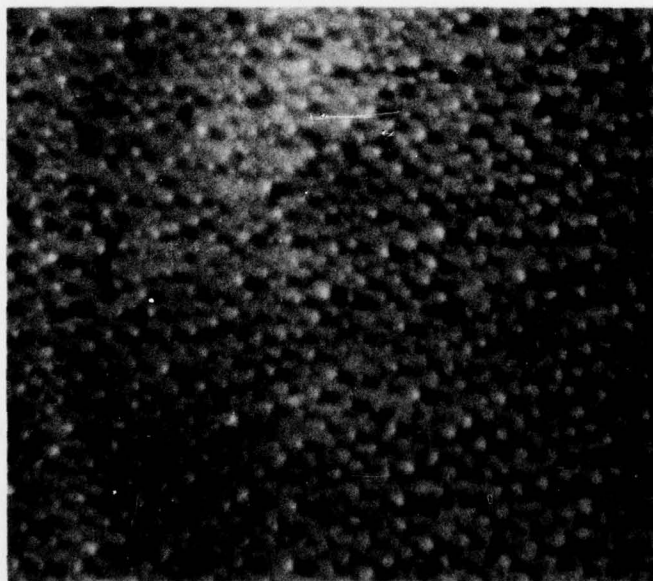
Figure 10.   Micrograph of RJ-5 droplets generated by ultrasonic nebulizer at 1.4 MHz; 1 mm = 2 μ

where $g = 980$ cm/sec^2

    d = droplet diameter

    ρ_p = density of droplets

    ρ_m = density of settling medium

    η_m = viscosity of settling medium

since the viscosity of air does not change significantly over this pressure range, and $\rho_m << \rho_p$. Although the origin of this effect is not clear, it can be overcome by mechanical or airjet mixing.

One area in which the literature is deficient concerning ultrasonic nebulizers is the lower liquid volume limit at which they efficiently operate. In fact, in most reported applications, the transducer was entirely submerged under a layer of liquid. We were concerned with this question because successful deployment of the initial shock tube design required the capability for nebulizing very small amounts of fuel ($<25\mu\ell$). Furthermore, the modifications required to accomodate large liquid volumes would not have been easy to implement. However, experiments showed that samples of liquid as small as 0.5 $\mu\ell$ could be easily nebulized inside the shock tube combustion chamber.

It is noteworthy that even very small amounts of RJ-5 lead to enormous numbers of fuel droplets. For instance, complete nebulization of a 5-$\mu\ell$ sample of RJ-5 with an average particle diameter of 5 microns would lead to 8×10^7 droplets. If these droplets were isolated in the last 100 cm^3 of the shock tube, the droplet density would be about 10^6 droplets/cm^3.

<u>Mist Combustion</u>

Having determined that a stable mist of fuel droplets could be successfully generated in the shock tube combustion chamber, we performed a series of experiments to demonstrate that heterogeneous fuel combustion was indeed occurring in the shock tube combustion chamber. The results of these experiments are depicted in the series of Polaroid records discussed below.

A preliminary shock wave was initiated into oxygen-containing RJ-5 mist. An explosion clearly took place, as evidenced by a loud noise and an intense visible flash (Figure 11) which emanated from the windows of the combustion chamber. An infrared detection system containing a narrow band filter to selectively monitor emissions from one product of combustion, CO_2, was then coupled to one viewing port. The opposite viewing
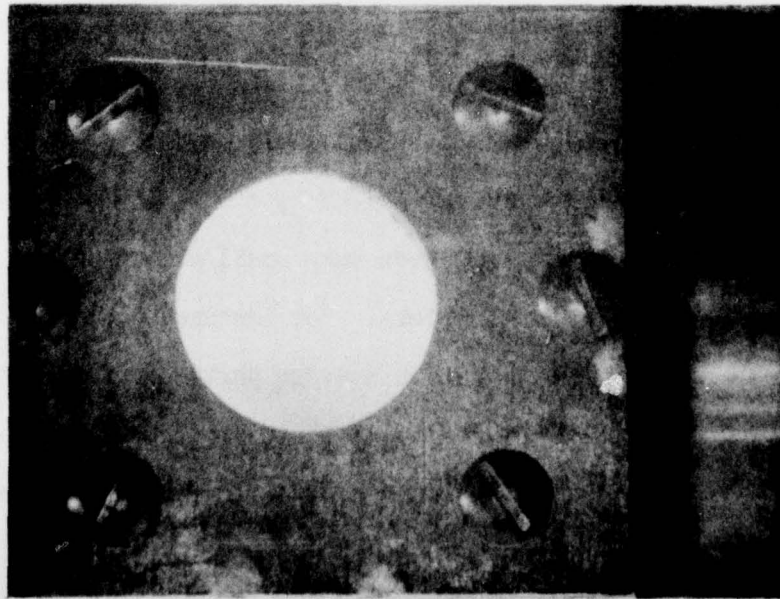
Figure 11.   Visible flash from RJ-5 combustion; visible light emitted during combustion experiment is indicated by white central spot.

26

port was equipped with a phototube assembly to detect the visible emissions during combustion. The signals from these two detectors, along with the signal from a pressure transducer, were simultaneously displayed on an oscilloscope for the remaining experiments. A detailed schematic of these monitoring devices has already been presented (Figure 7).

The purpose of the first fully implemented nebulizer-coupled shock tube experiment was to ascertain background visible and infrared emission levels for RJ-5 vapor combustion to be used as reference for the nebulizer experiments. This was essential since it would otherwise be impossible to distinguish with certainty vapor from droplet combustion. In this initial experiment, fuel was placed on the surface of the transducer but not nebulized; a shock wave was generated through O_2 saturated with RJ-5 vapor. The Polaroid record of this experiment is shown in Figure 12. At the signal sensitivities chosen, no visible light was observed in the milli-second observation time; however, there was a small but detectable signal in the infrared which was attributed to the small amount of RJ-5 vapor combustion. The pressure profile was steady throughout the entire time period, suggesting that extensive energy releasing reactions had not taken place.

Signal Intensity (0.5v/cm)

t_o Time (100 μsec/cm)
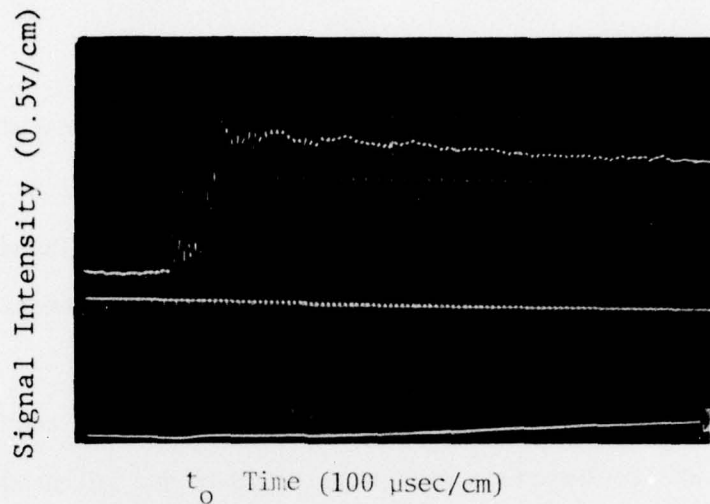
Figure 12.   Background emission levels for RJ-5 vapor combustion near 1500°K. Lower trace: infrared emission from CO_2; middle trace, visible emission; upper trace, pressure profile; t_o marks reflected shock arrival at observation station.

Following this vapor combustion experiment, the experiment was repeated with a small amount of liquid fuel nebulized to produce a low-density mist. The results of this experiment are shown in Figure 13. The appearance of both visible and infrared emissions shows clearly that mist ignition occurred after about 300 μsec, followed by a slow droplet burning. The infrared emission prior to this point was again mostly due to the very rapid burning of the RJ-5 already in the vapor phase.

Signal Intensity (0.5v/cm)

t_o Time (100 μsec/cm)
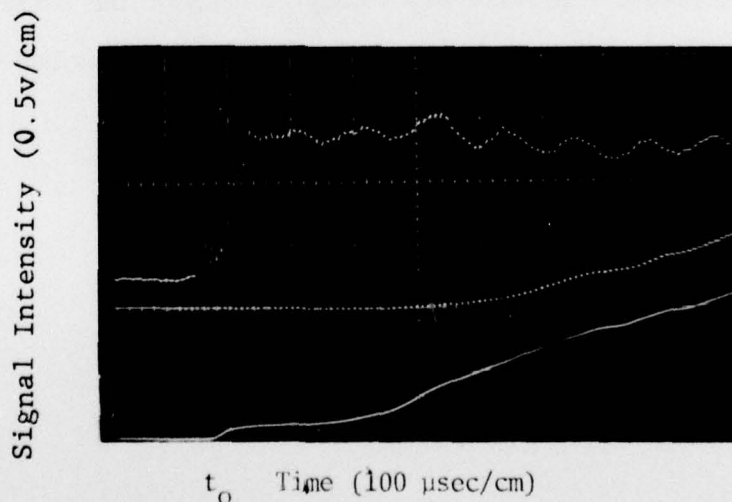
Figure 13.   Nebulized RJ-5 combustion experiment near 1500°K. Lower trace: infrared emission from CO_2; middle trace, visible emission; upper trace, pressure profile; t_o marks reflected shock arrival at observation station.

28

Figure 14 represents a repeat of the previous experiment with a slightly higher concentration of fuel droplets. The driver pressure was also increased slightly to obtain a higher initial temperature, and thus drive droplet combustion to completion. This had the effect of decreasing the droplet ignition delay to about 100 μsec. The amount of CO_2 produced was significantly increased, as is indicated by the increased infrared emission (note: the signal sensitivity for the infrared profile has been halved). Also, the signal leveled off, suggesting that combustion was complete. Furthermore, there was a pressure rise coincident with ignition, indicating that a large amount of fuel was now burning.

Signal Intensity (1.0 v/cm)

t_0 Time (100 μsec/cm).
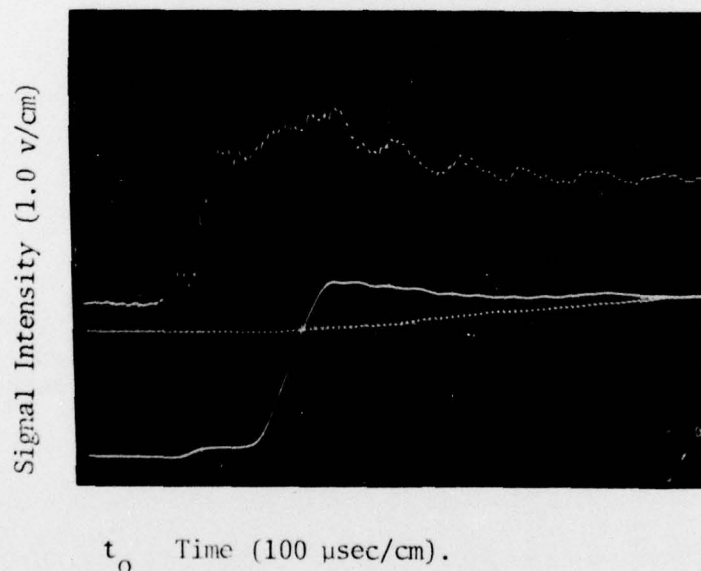
Figure 14.   Nebulized, low-density RJ-5 combustion near 1700°K. Lower trace: infrared emission from CO_2; middle trace, visible emission; upper trace, pressure profile; t_0 marks reflected shock arrival at observation station.

This experiment was once again repeated with the combustion chamber saturated with RJ-5 droplets. As can be seen in Figure 15, CO_2 production was further increased, and a large pressure pulse suggesting the occurrence of extensive combustion, was observed.

t$_0$ Time (100 μsec/cm)
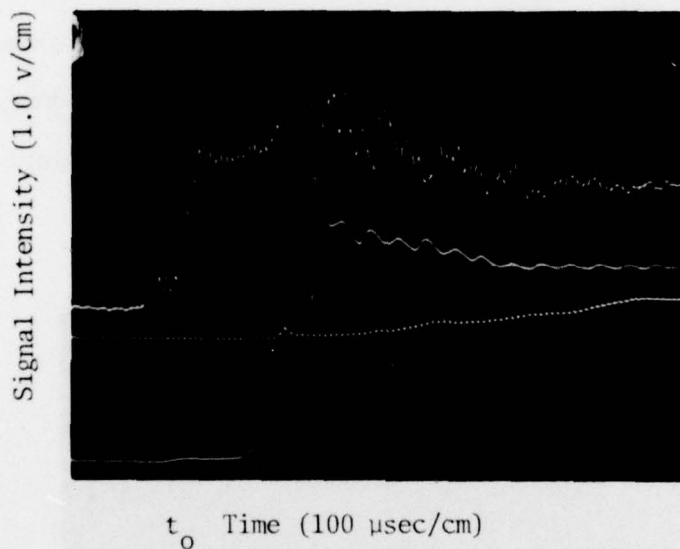
Figure 15. Nebulized, high-density RJ-5 combustion near 1700°K. Lower trace: infrared emission from CO_2; middle trace, visible emission; upper trace, pressure profile; t$_0$ marks reflected shock arrival at observation station.

The results of these experiments are typical of those obtained with the nebulizer-coupled shock tube. In all cases, vapor ignition coincided with reflected shock arrival (τ vapor <1 µsec) and was followed by ignition and combustion of the fuel droplets. The rapid vapor ignition was consistent with results from the first phase of this study.

In contrast to the vapor ignition, the ignition delay and combustion duration of the fuel drops were highly dependent upon temperature. Increasing the temperature from 1500 to 1700°K led to a decrease in ignition delay from 200 µsec to 100 µsec. The combustion duration was affected to an even greater extent. At 1700°K, CO_2 production ceased after approximately 100 µsec, whereas, at 1500°K, CO_2 formation was still occurring 500 µsec after ignition of the fuel drops.

In summary, the significant results from this work are:

- Fuel mist ignition and combustion can be induced in a chemical shock tube.

- The shock tube combustion of fuel mist can be monitored by infrared, visible, and pneumatic detectors.

- Fuel mist ignition delays are much longer than those of vapor.

- Ignition delays and combustion duration of fuel mist are significantly decreased by increasing temperature.

CONCLUSIONS AND RECOMMENDATIONS

The goal of kinetic studies of combustion is to provide sufficient insight into this phenomenon to assist in the design and use of systems deriving energy from fuel combustion. The problems encountered in these efforts are usually due to difficulties in extrapolating from laboratory-measured kinetic parameters to fuel performance in commercial devices, and arise from the failure of most laboratory experiments to adequately simulate practical conditions. In the present study, we have demonstrated that the high-temperature heterogeneous fuel mist-air environment of real systems can be simulated by using the nebulizer-coupled shock tube technique. Furthermore, infrared, visible, and pneumatic devices can be used to monitor the combustion process in situ. Although the results reported here are only preliminary, further refinements of the technique should yield results of direct relevance to real systems. We,therefor . recommend that support in this area continue until the technique is fully developed.